

Journal of Materials Chemistry B

Accepted Manuscript



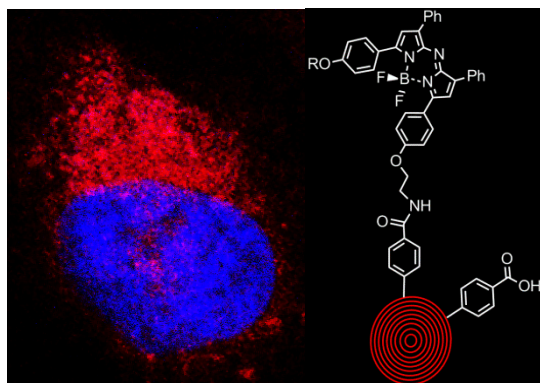
This is an *Accepted Manuscript*, which has been through the Royal Society of Chemistry peer review process and has been accepted for publication.

Accepted Manuscripts are published online shortly after acceptance, before technical editing, formatting and proof reading. Using this free service, authors can make their results available to the community, in citable form, before we publish the edited article. We will replace this *Accepted Manuscript* with the edited and formatted *Advance Article* as soon as it is available.

You can find more information about *Accepted Manuscripts* in the [Information for Authors](#).

Please note that technical editing may introduce minor changes to the text and/or graphics, which may alter content. The journal's standard [Terms & Conditions](#) and the [Ethical guidelines](#) still apply. In no event shall the Royal Society of Chemistry be held responsible for any errors or omissions in this *Accepted Manuscript* or any consequences arising from the use of any information it contains.

TOC



The synthesis and characterisation of hybrid carbon nano-onion materials which are surface conjugated with NIR fluorescent boron difluoride azadipyrromethenes is described. These new nano-construct retain the strong NIR fluorescence properties of the fluorophore and have the ability to be reversibly switch emission output on and off in response to pH changes. These NIR fluorescence properties are demonstrated both in solution and intracellularly. The image shows carbon nano-onions (red) inside HeLa cells (cell nucleus is blue).

ARTICLE

NIR Fluorescence Labelled Carbon Nano-Onions: Synthesis, Analysis and Cellular Imaging

Cite this: DOI: 10.1039/x0xx00000x

Silvia Giordani,^{*a} Juergen Bartelmess,^a Marco Frasconi,^a Ilaria Biondi,^b Shane Cheung,^b Marco Grossi,^b Dan Wu,^b Luis Echegoyen,^c Donal F. O'Shea^{*b}

Received 00th January 2012,

Accepted 00th January 2012

DOI: 10.1039/x0xx00000x

www.rsc.org/

The preparation of novel NIR fluorescent carbon based nanomaterials, consisting of boron difluoride azadipyromethene fluorophores covalently attached to carbon nano-onions, is demonstrated. In addition, the analysis of the new nanomaterial is presented. The fluorescent nano-derivative properties are customized such that their emission can be reversible on/off modulated in response to pH, which is demonstrated in solution and in cells. *In vitro* imaging of HeLa Kyoto cells is carried out and the cellular uptake of the carbon nano-onion NIR fluorophore conjugates is verified.

Introduction

Nano-platforms capable of carrying therapeutic agents as well as producing an optical output in recognition of a specified target for imaging hold great potential in the treatment of cancer and other diseases.^{1,2} Despite much interest in other carbon-based nano-materials, multi-shell fullerenes, known as carbon nano-onions (CNOs), as functional constructs for intracellular transport have not yet been explored. CNOs, discovered in 1992, are structured by concentric shells of carbon atoms.^{3,4} They display several unique properties, such as a large surface area to volume ratio, a low density and a graphitic multilayer morphology.^{5,6}

Initial investigations of the effects of large CNOs (diameter of approximately 30 nm) on the immune system indicated that the cell response was highly dependent on the structure of the carbon nanomaterial.⁷ We recently reported the weak inflammatory potential and low cytotoxicity *in vitro* and *in vivo* of small surface functionalized CNOs (diameter of approximately 5 nm) and their ability to be up-taken by antigen displaying cells, demonstrating that the inflammatory properties of the CNOs can be controlled by the chemical functionalities present on their surface.⁸ These promising biological results led us to investigate the development of novel intracellular imaging systems based on CNOs, with special attention to the biologically important near-infrared (NIR) region.⁹ Absorption and emission in the NIR region is of great importance for applications in biology, as NIR light has dramatically lower light induced cellular toxicity than shorter wavelengths and is more effectively transmitted through body tissue. NIR

fluorescence imaging is an inexpensive and non-invasive technique with potential for use in real-time.¹⁰ In addition to our study using fluorescein labelled CNOs,⁸ there are only two other reports on the use of CNOs for biological imaging: the group of Sarkar used water-soluble, defect rich, oxidized CNOs, synthesized from wood waste, for imaging the life cycle of *Drosophila melanogaster*¹¹ and to study *Escherichia coli* and *Caenorhabditis elegans*.¹²

Boron difluoride azadipyromethenes are a relatively new class of NIR fluorophores with emerging biological and medicinal applications.^{13,14,15} They are also used for molecular sensing,^{16,17} as building blocks in light-harvesting systems^{18,19,20,21,22} and they have been successfully employed for the functionalization of carbon nanotubes.^{23,24}

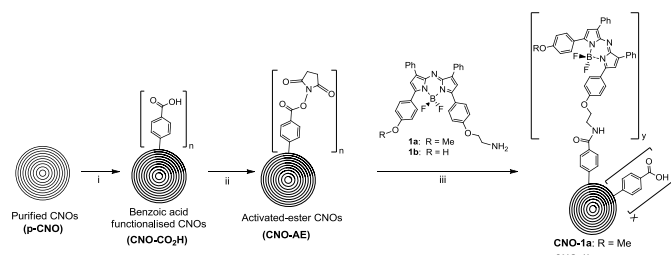
In this study, we report the first synthesis and characterization of near infrared active boron difluoride azadipyromethene²⁵ functionalized CNOs and we investigate their uptake in HeLa Kyoto cells. We demonstrate that the NIR-fluorophore is able to retain emissive properties when conjugated to the CNOs and upon internalization by cells. Importantly, we report that the NIR-emission of the nanoparticles can be on/off modulated in response to pH both in solution and in the cells.

Results and Discussion

Synthesis

The synthetic procedure used to prepare CNO-NIR fluorophore nanoparticles is illustrated in Scheme 1; detailed synthetic procedures can be found in the ESI. Pristine CNOs (**p-CNO**) were covalently functionalized using the one-pot Tour reaction

comprising 4-aminobenzoic acid and isoamyl nitrite to produce benzoic acid functionalized and dispersible **CNO-CO₂H**,²⁶ that were then converted to the corresponding electrophilic activated ester intermediate **CNO-AE** by activation with *N*-hydroxysuccinimide. The synthesis of NHBoc-protected boron difluoride azadipyromethene derivative Boc-**1a** was previously published¹⁰ and Boc-**1b** was synthesized as described in the ESI. Following Boc deprotection, amino functionalized NIR-fluorophores **1a** and **1b** were reacted with **CNO-AE** in DMF at RT for 72 hours. Then, the non-covalently bound fluorophore was removed from **CNO-1a** and **CNO-1b** by repeated dispersion of the particles in DMF and centrifugation until the supernatant was no longer fluorescent.



Scheme 1 (i) 4-Aminobenzoic acid, isoamyl nitrite, DMF, 60 °C, 24 h, N₂ (ii) NHS, EDC-HCl, DIPEA, DMF, RT 48 h (iii) DIPEA, DMF, RT, 72 h.

Characterization of NIR-fluorescent CNO nanoparticles

The functionalized carbon nano-onions were characterized by a number of techniques, including thermogravimetric analysis (TGA), Raman, fourier transform infrared (FTIR), absorption and emission spectroscopy as well as atomic force microscopy (AFM) and high resolution transmission electron microscopy (HRTEM) (Figure 1).

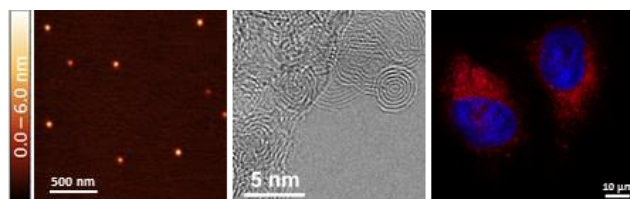


Figure 1 AFM (left), HRTEM (centre) and confocal microscopy (right) images of **CNO-1a** (red colour), internalized in HeLa Kyoto cells in the case of the confocal microscopy image. (scale bar 10 μM).

The TGA analysis confirms the successful covalent functionalization of the **CNO-1a** (Figure S1 in the ESI). The CNO decomposition temperature under air is lowered upon covalent functionalization, a result in line with earlier studies.^{8,26} An increased weight loss of **CNO-1a** at lower temperatures, between 200°C and 400°C, verifies the presence of additional organic functionalities, the boron difluoride azadipyromethene fluorophore. The degree of functionalization of the CNO nanomaterial was estimated from the weight losses, as described in the literature,²⁷ assuming that one CNO consists of 6 graphitic shells. The TGA of **CNO-CO₂H** and **CNO-1a** performed in air show a weight loss at 400°C of about 10% and 17% respectively. We estimated about

55 benzoic acid functionalities per onion for **CNO-CO₂H** and approx. 21 boron difluoride azadipyromethene molecules per CNO for **CNO-1a**. This degree of functionalization leaves some benzoic acid functionalities, about 34 units, on the surface of the CNO, providing additional water-solubility for the CNO-NIR fluorophores conjugate.

Raman spectroscopy was used to follow the progress of the CNO functionalization (Figure S6 in the ESI) and illustrates an increase of the CNO D-band, relative to the G-band, corroborating the successful covalent functionalization. The D/G-band ratio of the p-CNO is about 1.23 and increases upon functionalization to 1.56 for **CNO-CO₂H** and to 1.91 for **CNO-AE**. In the Raman spectrum of **CNO-1a**, a strong background fluorescence signal is observed (Figure S7 in the ESI), which is caused by the emission of the boron difluoride azadipyromethene at the excitation wavelength of 632 nm.

FTIR spectroscopy was used as an additional technique to follow the functionalization of CNOs, firstly with benzoic acid, which was then activated with *N*-hydroxysuccinimide (Figure S8 in the ESI). Also the successful subsequent functionalization with boron difluoride azadipyromethene **1a** could be corroborated by FTIR spectroscopy (Figure S9 in the ESI). The IR spectrum of **CNO-1a** displays some IR bands similar to the ones found in the IR spectra of Boc-**1a**. This includes IR bands in the aromatic region at 3000 cm⁻¹. At lower wavenumbers, **CNO-1a** reveals several IR absorption bands between 600 and 1600 cm⁻¹, which can be assigned to the presence of the boron difluoride azadipyromethene fluorophore. Some resemblance to the IR bands of **1a** is obvious, but the strong background absorption of the CNO bulk material makes it impossible to clearly identify and assign certain IR bands to specific functionalities. Nevertheless, the presence of additional IR absorption bands (when compared to those of **CNO-AE** for example), is a further indication that a successful functionalization with boron difluoride azadipyromethene fluorophores **1a** has been achieved.

The presence of the fluorophore is also evident from the absorption spectrum of **CNO-1a** (Figure 2 - inset), where a broadening of the boron difluoride azadipyromethene absorption bands can be observed upon CNO functionalization. The broad background absorption observed in the absorption spectrum of **CNO-1a** is typical for nanocarbon materials.^{8,23,24,26}

The boron difluoride azadipyromethene derivatives Boc-**1a**⁹ and Boc-**1b** were chosen as reference NIR fluorophores, since their molecular structure (Boc-protected amine group) is closely related to the CNO bound boron difluoride azadipyromethene. The spectroscopic properties of Boc-**1a** and Boc-**1b** are summarized in detail within the ESI.

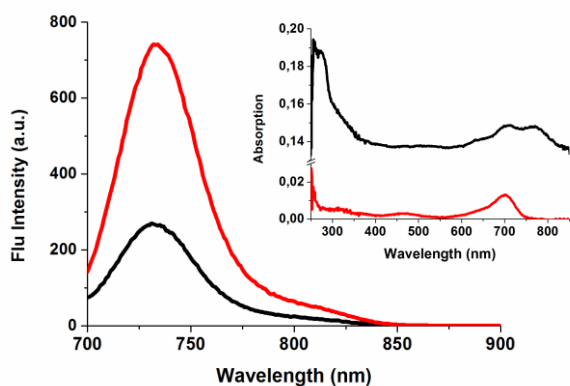


Figure 2 Emission spectra of Boc-1a (red line) and CNO-1a (black line) that exhibit the same optical density of the fluorophore at the excitation wavelength. Inset: Absorption spectra of boron difluoride azadipyromethene derivative Boc-1a (red line) and CNO-1a (black line). (Solvent: DMSO, λ_{exc} = 690 nm).

Comparison of the fluorescence features of the boron difluoride azadipyromethenes derivative Boc-1a and CNO-1a, at an excitation wavelength of 690 nm in DMSO, shows a reduced fluorescence intensity of the CNO conjugate while the absorption of the boron difluoride azadipyromethenes at the excitation wavelength of both samples was comparable (Figure 2). A plausible explanation for this observation is the high background absorption of the CNOs. Comparing the maximum fluorescence intensities, the fluorescence quantum yield of CNO-1a can be estimated to be about one third of the reference fluorophore Boc-1a (about 0.08 for CNO-1a vs. 0.25 for Boc-1a). The fluorescence lifetime of Boc-1a in DMSO is 2.7 ns, while upon attachment to the CNOs, the fluorescence lifetime of the NIR emission decreases slightly to 2.5 ns for CNO-1a. In addition, the emission maximum of CNO-1a is observed at 731 nm, while reference compound Boc-1a has a fluorescence maximum of 735 nm. This small shift further corroborates a successful functionalization of the CNO with boron difluoride azadipyromethene 1a. When comparing the observation of a reduced, but not fully quenched fluorescence emission, with earlier studies of single wall-carbon nanotubes (SWNTs), functionalized with similar boron difluoride azadipyromethene derivatives, the SWNT based systems show a much larger, almost quantitative fluorescence quenching.^{23,24} In a previous study, we were able to show that this fluorescence quenching in SWNT-boron difluoride azadipyromethene conjugates was due to electron transfer from the photo-excited NIR fluorophore to the SWNTs.²³ However, in the present system, we attribute the reduction of the fluorescence emission to the strong absorption of the CNO and not to other photophysical effects. The near quantitative fluorescence quenching of fluorophores covalently linked to carbon nanomaterials is a widespread problem and greatly restricts the use of these hybrid materials for biological applications.^{28,29,30} Fortunately, this problem is dramatically reduced in these new CNO based nanomaterials. This is one of the key important aspects of the presented work. The modulation of NIR fluorescence in response to pH for the

previously unreported phenolic substituted Boc-1b was clearly observable upon titration from pH 6.0 to 9.0 (Figure 3). In the lower physiological pH range the phenolic fluorescence switch controller is protonated resulting in a high intensity NIR emission but upon deprotonation to the phenolate at higher pH the emission is virtually quenched completely.

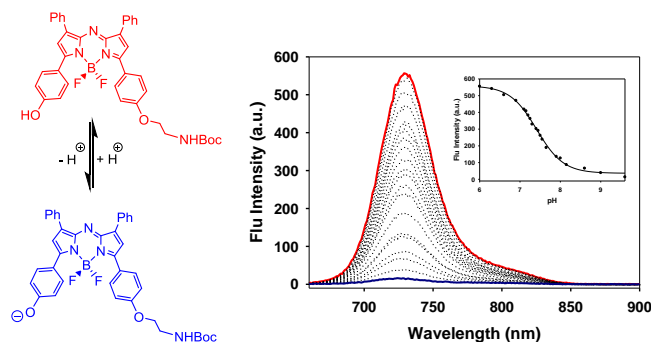


Figure 3 Emission spectral changes for Boc-1b between pH 6.0 (red line) and 9.6 (blue line) at 1×10^{-7} M in water/CRFL. I_{NaCl} = 150 mmol/L.

These titration results showed a highly efficient on/off switching for Boc-1b with a fluorescence enhancement factor (FEF) of >30 and an apparent pKa of 7.3. It would be remarkable if this molecular on/off switching mechanism controlled by the phenol/phenolate inter-conversion could be maintained after its covalent linkage to the CNO (Figure 4A).

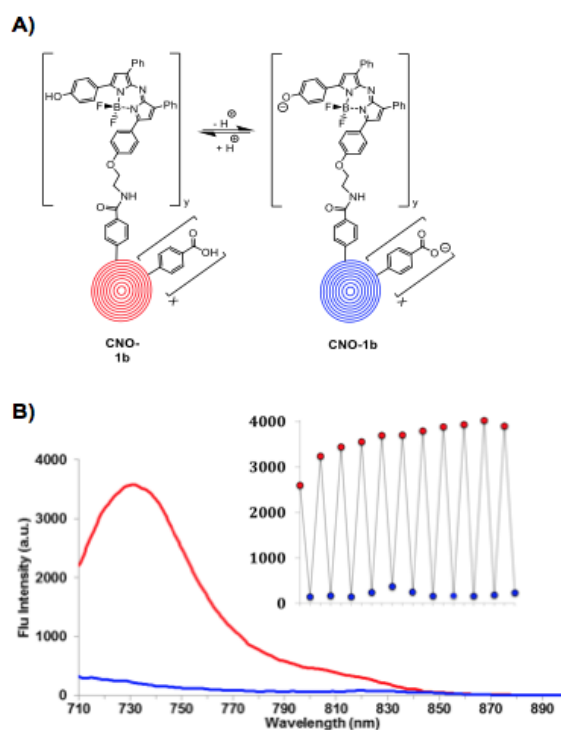


Figure 4 (A) Schematic representation of "on"/ "off" switching of CNO-1b. (B) Emission spectra of CNO-1b when protonated (red line) and deprotonated (blue line). Inset: modulation of CNO-1b emission at 729 nm with addition of DBU cycles of TFA and DBU (0.1 mg/mL in DMSO; λ_{exc} = 690 nm).

The switching ability of the **CNO-1b** was investigated by monitoring changes in the emission upon alteration between phenol and phenolate states in DMSO by the addition of trifluoroacetic acid (TFA) or 1,8-diazabicyclo[5.4.0]undec-7-ene (DBU), respectively. The emission spectra shown in Figure 4B clearly demonstrate the switching, where the characteristic fluorophore emission band is evident (red line) and disappears immediately upon addition of DBU base (blue line), indicating almost quantitative quenching of the excited state. The on/off switching of the excited state of **CNO-1b** is completely reversible, where modulation or cycling of the emission band at 729 nm, following repeat additions of aqueous acid (TFA) and base (DBU), is shown in the inset.

Cytotoxicity Studies

In order to study the suitability of the fluorescent CNOs for cellular imaging, the cytotoxicity of the modified CNOs was tested on HeLa cells. Previous *in vitro* and *in vivo* studies of surface functionalized CNOs showed weak inflammatory properties and low cytotoxicity of CNOs.⁸ In the current study, cells were treated with **CNO-CO₂H**, **CNO-AE**, **CNO-1a** and **CNO-1b** at various concentrations. Time dependence viability of the treated cells was quantified by using a resazurin-based assay, PrestoBlue™ (see ESI for experimental details). Cells treated with only a cell culture media were used as a control, and the CNO samples were compared to this control.

Cell viability is not significantly affected by the **CNO-1a** up to concentration of at least 100 µg/mL for 72h of incubation (Figure 5). A similar non-toxic behaviour was observed for the other fluorophore modified CNOs, **CNO-1b**, and the benzoic acid functionalized CNOs, **CNO-CO₂H**, while a significant reduction of the cell viability was detected for the **CNO-AE** at 100 µg/mL.

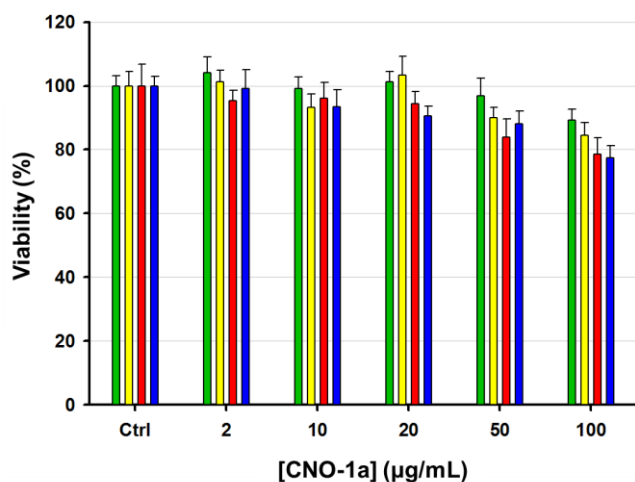


Figure 5 Viability of HeLa cells 12h (green bar), 24h (yellow bar), 48h (red bar) and 72h (blue bar) after the exposure to increasing doses (2; 10; 20; 50; 100 µg/mL) of **CNO-1a**. Viability of the treated cells is expressed relative to non-treated control cells, as the mean and the standard error of the mean of three experiments.

Collectively these results demonstrate that the chemical surface functionalization of the carbon nanomaterial critically effect the toxicity of the CNOs and the high viability of the investigated nanomaterials allows for a safe use of the fluorophore functionalized CNOs as imaging agents.

Cell Imaging

HeLa cells were incubated at 37 °C with **CNO-1a** for 2 hours, washed, fixed with paraformaldehyde and imaged using laser scanning confocal microscopy (LSCM). Figure 6 illustrates that **CNO-1a** has been internalised by HeLa Kyoto cells, as a clear NIR fluorescence is observed with emission being more intense in the perinuclear region, which suggests the CNOs are internalised by endocytosis and trafficked by lysosomes.

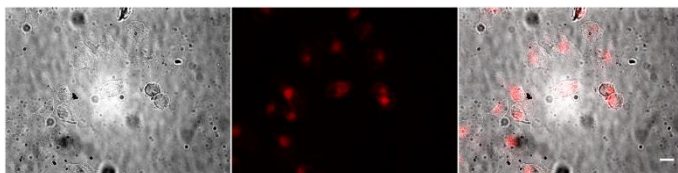


Figure 6 Phase contrast image of HeLa Kyoto cells incubated with **CNO-1a** (left), fluorescence image of the same field of view using a Cy5 filter (middle) and phase contrast/fluorescence overlay (right). (50 µg/mL of DMSO **CNO-1a** in DMEM. All images acquired at 63X. Scale bar 10 µm).

In order to confirm that the particles were internalised by the cells and not just localized on the plasma membrane, cells nuclei were stained blue with Hoechst 33342 and optical sectioning of the cells with laser scanning confocal microscopy (LSCM) was performed. Acquiring a z-stack by optical sectioning adds a third dimension of analysis, which proves that the fluorescent CNOs are distributed throughout the cytosol (Figure 7).

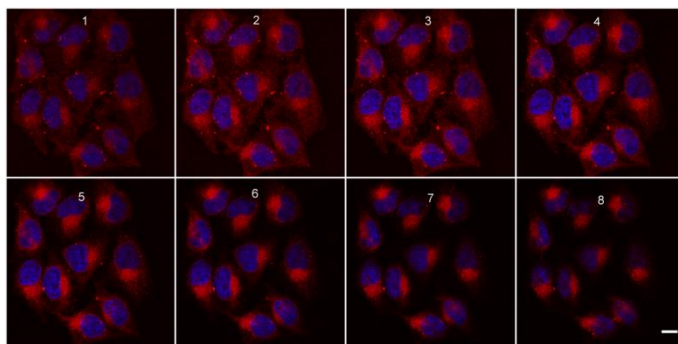


Figure 7 Eight optical slices of HeLa Kyoto cells incubated with **CNO-1a** (left), taken through the z-axis. Images 1-8 from the bottom of the cell to the top. Nuclei stained blue with Hoechst 33342. (Scale bar 10 µm).

To illustrate the pH response of **CNO-1b** *in vitro*, HeLa cells were incubated with a **CNO-1b** dispersion (50 µg/mL) in DMEM for two hours and fixed. After fixing, the cells were imaged and it was observed that **CNO-1b** had been successfully internalised by the cells and, as expected, were fluorescent at physiological pH. To determine if the pH responsive **CNO-1b** retained its ability to turn fluorescence off and on intracellularly, the pH of two imaging wells were

adjusted to 8.5 and 4.5 and re-imaged. Gratifyingly, a strong NIR emission intensity was clearly seen in the cells at pH 4.5 (Figure 8, right) when compared to a weak trace NIR emission at pH 8.5 (Figure 8, left). Confocal z-stacks of cells containing **CNO-1b** confirmed that the CNOs were internalized by the cell.

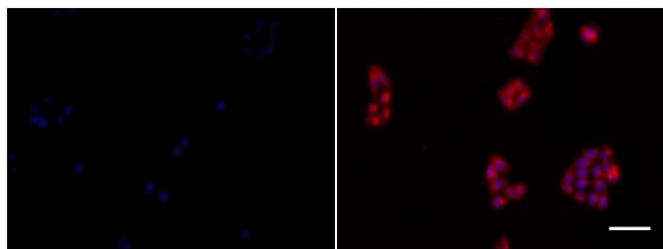


Figure 8 Fluorescence images of fixed HeLa Kyoto cells incubated with **CNO-1b** at pH 8.5 (left), and 4.5 (right). Nuclei stained blue with DAPI. Imaged at 20x magnification, scale bar 100 μ m.

Conclusions

In summary, boron difluoride azadipyromethene functionalized CNO conjugates have been synthesised and characterised. The NIR fluorescence properties of the difluoride azadipyromethenes are maintained after covalent linking to the CNO, allowing for intracellular identification with LSCM imaging. The ability to reversibly switch on and off the NIR fluorescence by the pH controlled phenol/phenolate modulation of the fluorophore linked CNOs was demonstrated both in solution and *in vitro*. This ability to report on environmental changes *in vitro* offers significant scope for the development of smart responsive CNO constructs. Further surface functionalization of the CNOs is ongoing to allow for the incorporation of targeting moieties as well as for drug delivery systems, potentially leading to tailor-made theranostic nanomaterials.

Acknowledgements

The authors wish to thank Adrian Villalta-Cerdas (University of Texas at El Paso) for CNO synthesis, Giammarino Pugliese (IIT) for TGA measurements, Nicola Pesenti for AFM and Rosaria Brescia (IIT) for HRTEM. Istituto Italiano di Tecnologia and Science Foundation Ireland are greatly acknowledged for research funding. We also thank the Department of Nanochemistry at IIT for cell culture facility. DW thanks China Scholarship Council for a Ph.D. fellowship. LE wished to thank the US NSF, PREM Program (DMR-1205302) and the Robert A. Welch Foundation (Grant AH-0033) for generous support.

Notes and references

^a Istituto Italiano di Tecnologia (IIT), Nano Carbon Materials, Via Morego 30, 16163 Genova, Italy.
E-mail: silvia.giordani@iit.it

^b Department of Pharmaceutical and Medicinal Chemistry, Royal College of Surgeons in Ireland, 123 St. Stephen's Green, Dublin 2; School of

Chemistry and Chemical Biology, University College Dublin, Belfield, Dublin 4, Ireland.

Email: donalfoshea@rcsi.ie

^c Department of Chemistry, University of Texas at El Paso, El Paso, Texas, U.S.A

Electronic Supplementary Information (ESI) available: Various procedures, TGA results, additional spectroscopy and discussion. See DOI: 10.1039/b000000x/

- C. Fabbro, H. Ali-Boucetta, T. Da Ros, K. Kostarelos, A. Bianco and M. Prato, *Chem. Commun.* 2012, **48**, 3911-3926.
- B. S. Wong, S. L. Yoong, A. Jagusiak, T. Panczyk, H. K. Ho, W. H. Ang and G. Pastorin *Adv. Drug Delivery Rev.* 2013, **65**, 1964-2015.
- D. Ugarte *Nature* 1992, **359**, 707-709.
- D. Ugarte *Carbon* 1995, **33**, 989-993.
- J. L. Delgado, M. A. Herranz and N. Martin *J. Mater. Chem.* 2008, **18**, 1417-1426.
- A. Molina-Ontoria, M. N. Chaur, M. E. Plonska-Brzezinska and L. Echegoyen *Chem. Commun.* 2013, **49**, 2406-2408.
- L. Ding, J. Stülwell, T. Zhang, O. Elboudwarej, H. Jiang, J. P. Selegue, P. A. Cooke, J. W. Gray and F.F. Chen *Nano Lett.* 2005, **5**, 2448-2464.
- M. Yang, K. Flavin, I. Kopf, G. Radics, C. H. A. Hearnden, G. J. McManus, B. Moran, A. Villalta-Cerdas, L. A. Echegoyen, S. Giordani and E. C. Lavelle *Small* 2013, **9**, 4194-4206.
- R. Wang and F. Zhang *J. Mater. Chem. B* 2014, **2**, 2422-2443.
- A. Palma, L. A. Alvarez, D. Scholz, D. O. Frimannsson, M. Grossi, S. J. Quinn and D. F. O'Shea *J. Am. Chem. Soc.* 2011, **133**, 19618-19621.
- M. Ghosh, S. K. Sonkar, M. Saxena and S. Sarkar *Small* 2011, **7**, 3170-3177.
- S. K. Sonkar, M. Ghosh, M. Roy, A. Begum and S. Sarkar *Mater. Exp.* 2012, **2**, 105-114.
- D. O. Frimannsson, M. Grossi, J. Murtagh, F. Paradisi, D. F. O'Shea *J. Med. Chem.* 2010, **53**, 7337-7343.
- D. Wu and D. F. O'Shea *Org. Lett.* 2013, **15**, 3392-3395.
- P. Batat, M. Cantuel, H. Jonusauskas, L. Scarpantonio, A. Palma, D. F. O'Shea and N. D. McClenaghan *J. Phys. Chem. A* 2011, **115**, 14034-14039.
- A. Palma, M. Tasiar, D. O. Frimannsson, T. T. Vu, R. Méallet-Renault and D. F. O'Shea *Org. Lett.* 2009, **11**, 3638-3641.
- J. Murtagh, D. O. Frimannsson and D. F. O'Shea *Org. Lett.* 2009, **11**, 5386-5389.
- M. Yuan, X. Yin, H. Zheng, C. Ouyang, Z. Zuo, H. Liu and Y. Li *Chem. - Asian J.* 2009, **4**, 707-713.

-
- ¹⁹ S. Y. Leblebici, L. Catane, D. E. Barclay, T. Olson, T. L. Chen and B. Ma *ACS Appl. Mater. Interfaces* 2011, **3**, 4469-4474.
- ²⁰ A. N. Amin, M. E. El-Khouly, N. K. Subbaiyan, M. E. Zandler, S. Fukuzumi and F. D'Souza *Chem. Commun.* 2012, **48**, 206-208.
- ²¹ V. Bandi, K. Ohkubo, S. Fukuzumi and F. D'Souza *Chem. Commun.* 2013, **49**, 2867-2869.
- ²² V. Bandi, M. E. El-Khouly, K. Ohkubo, V. N. Nesterov, M. E. Zandler, S. Fukuzumi and F. D'Souza *J. Phys. Chem. C* 2014, **118**, 2321-2332.
- ²³ K. Flavin, K. Lawrence, J. Bartelmess, M. Tasior, C. Navio, C. Bittencourt, D. F. O'Shea, D. M. Guldi and S. Giordani *ACS Nano* 2011, **5**, 1198-1206.
- ²⁴ K. Flavin, I. Kopf, J. Murtagh, M. Grossi, D. F. O'Shea and S. Giordani *Supramol. Chem.* 2011, **24**, 23-28.
- ²⁵ S. O. McDonnell, M. J. Hall, L. T. Allen, A. Byrne, W. M. Gallagher and D. F. O'Shea *J. Am. Chem. Soc.*, 2005, **127**, 16360-16361.
- ²⁶ K. Flavin, M. N. Chaur, L. Echegoyen and S. Giordani *Org. Lett.*, 2009, **12**, 840-843.
- ²⁷ C. T. Cioffi, A. Palkar, F. Melin, A. Kumbhar, L. Echegoyen, M. Melle-Franco, F. Zerbetto, G. M. A. Rahman, C. Ehli, V. Sgobba, D. M. Guldi and M. Prato *Chem. Eur. J.* 2009, **15**, 4419-4427.
- ²⁸ V. V. Didenko, V. C. Moore, D. S. Baskin and R. E. Smalley *Nano Lett.* 2005, **5**, 1563-1567.
- ²⁹ B. Tian, C. Wang, S. Zhang, L. Feng and Z. Liu *ACS Nano* 2011, **5**, 7000-7009.
- ³⁰ Y. Liu, C.-y. Liu and Y. Liu *Appl. Surf. Sci.* 2011, **257**, 5513-5518.